Quasi-periodic variability of X-ray binaries and Active Galactic Nuclei – the Lense-Thirring precession model

Piotr Życki

CAMK PAN, Warsaw, POLAND

with: B. You, M. Bursa, C. Done, A. Ingram, M. Sobolewska, A. Niedźwiecki

Szczecin, 4.06.2024

„Galactic Nuclei in the Cosmological Context"

QPO in X-ray binaries and Active Galactic Nuclei

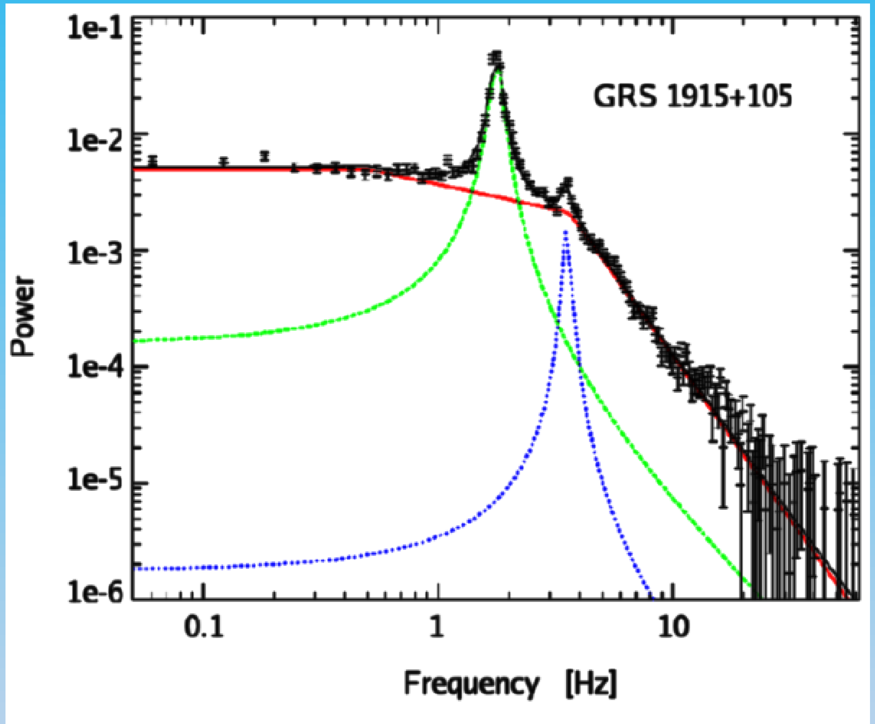

RE J1034+396

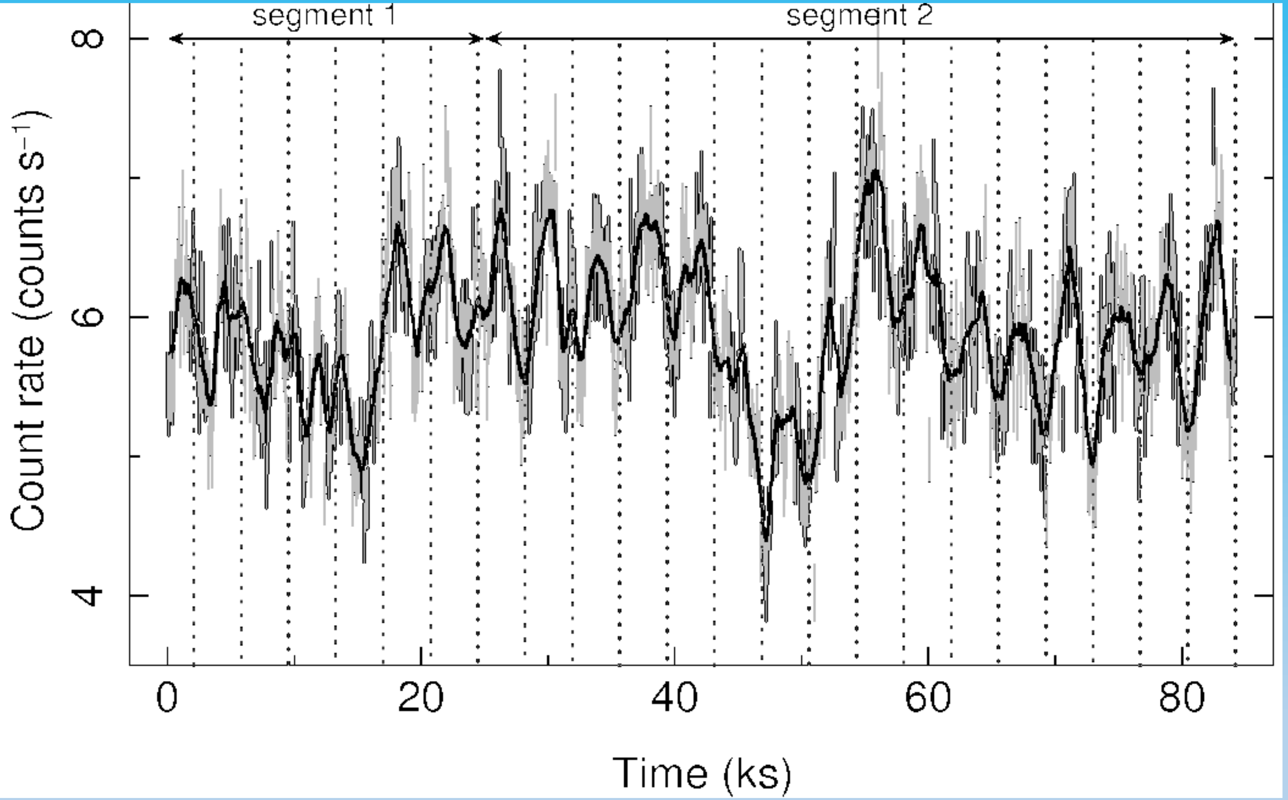

Gierliński et al., 2008, Nature

Low- and high- frequency QPO in XRB

HF QPO: hundreds of Hz

LF QPO: 0.1—10 Hz

High-frequency QPO

Rarely seen
Sometimes come in pairs, with 3:2 frequency ratio
Resonance frequency models, based on the 3:2 *f* ratio

What is the mechanism of X-ray modulation in these models?

Models are not yet advanced enough to answer this question

Resonance-frequency models

In the simplest version the assumption was that the intrinsic emission does not change and the variability is due to varying strength of the relativistic effects.

Studied in Bursa et al. (2004); Życki, Niedźwiecki, Sobolewska (2007); recent review in Smith, Tandon & Wagoner (2021)

Energy spectra of the QPO:

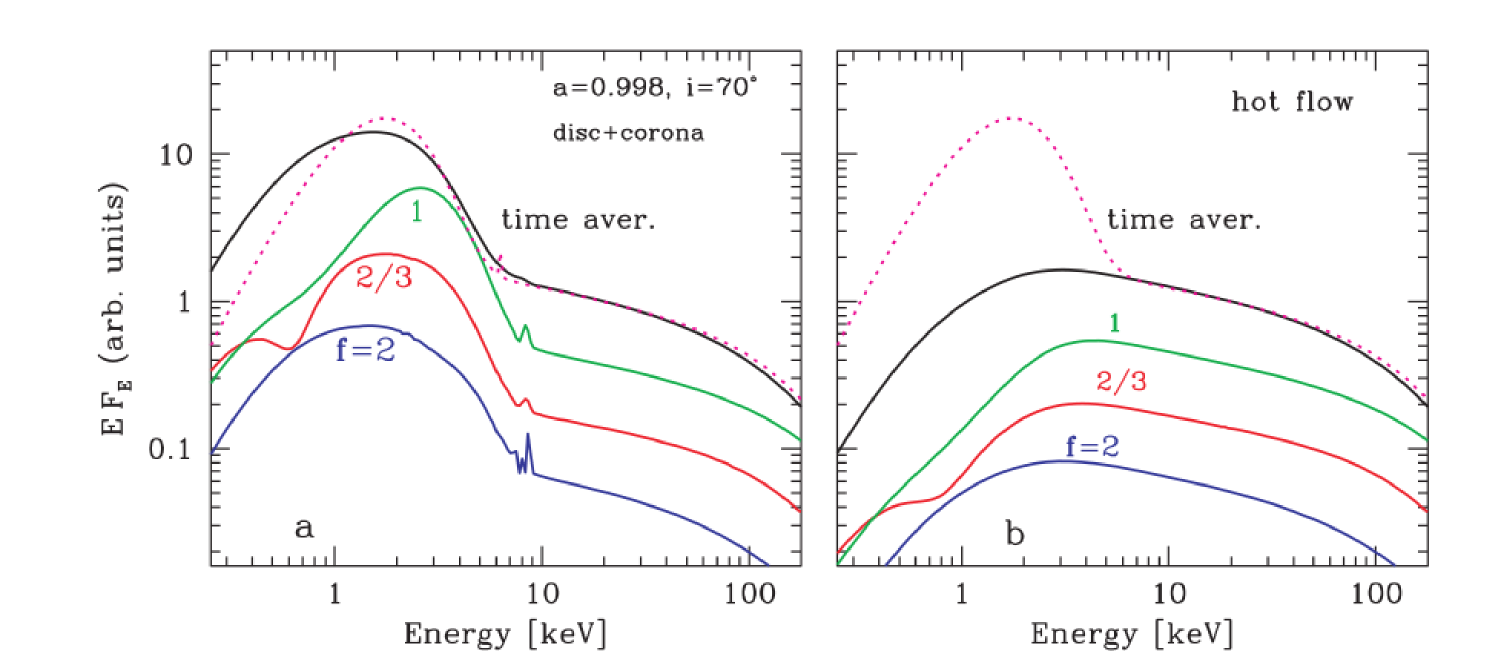

Resonance-frequency models

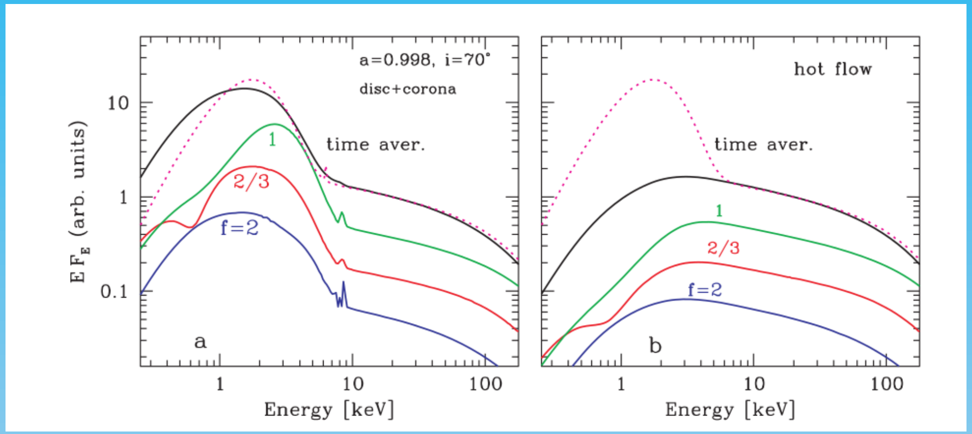

Observations: energy dependencies
e.g. GRO J1655-40: 300 Hz QPO seen in soft band (2-12 keV)
450 Hz QPO seen in hard band (13-24 keV)

How do we get different energy dependencies for different QPO in the 3:2 pair?

Low-frequency QPO

Data exist on spectral-temporal properties:

Disk emission not present in the QPO spectra – only the Comptonized component varies

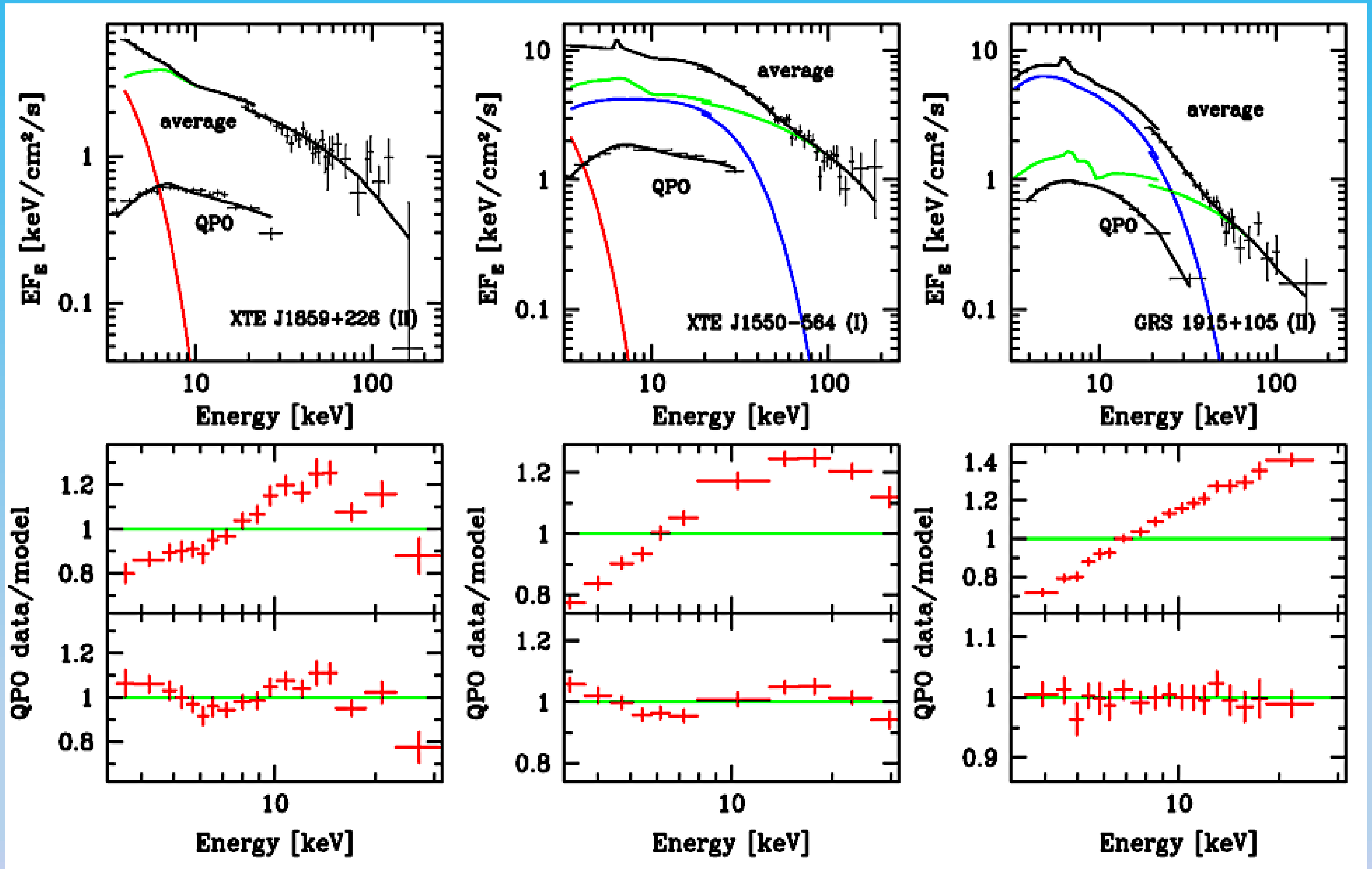

Sobolewska, Życki 2006

QPO in Active Galactic Nuclei

RE J1034+396

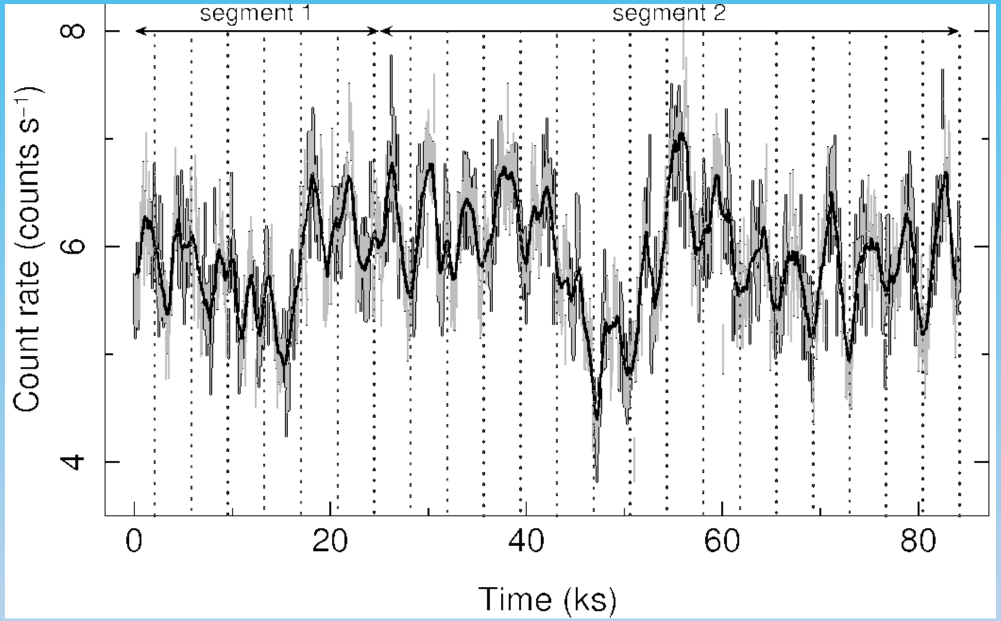

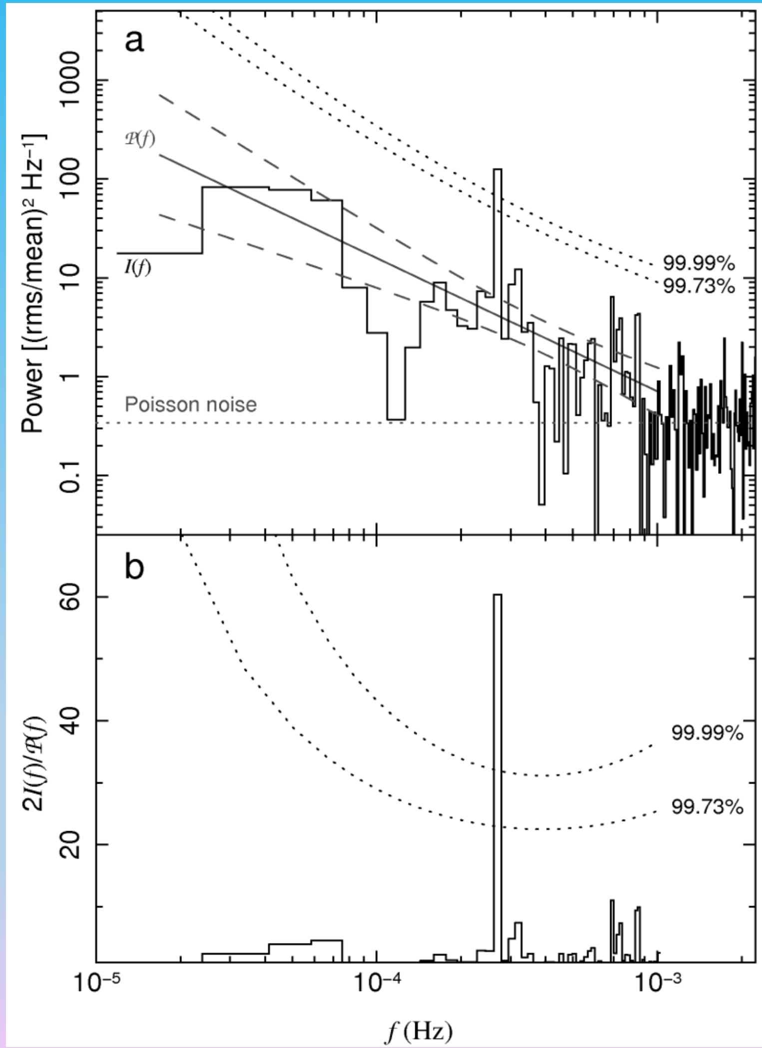

$f \sim 2.7\times10^{-4}$ Hz

T ~ 1 hour

Gierliński et al., 2008, Nature

QPO in RE J1034+396 – low-*f* or high-*f* ?

Black hole mass in RE J1034+396:
10^6 - 10^7 M_{SUN}
(Czerny et al., 2016)

It's most likely to be equivalent to the **67 Hz** QPO in GRS 1915+105 [then mass **3×10^6 M_{SUN}**]

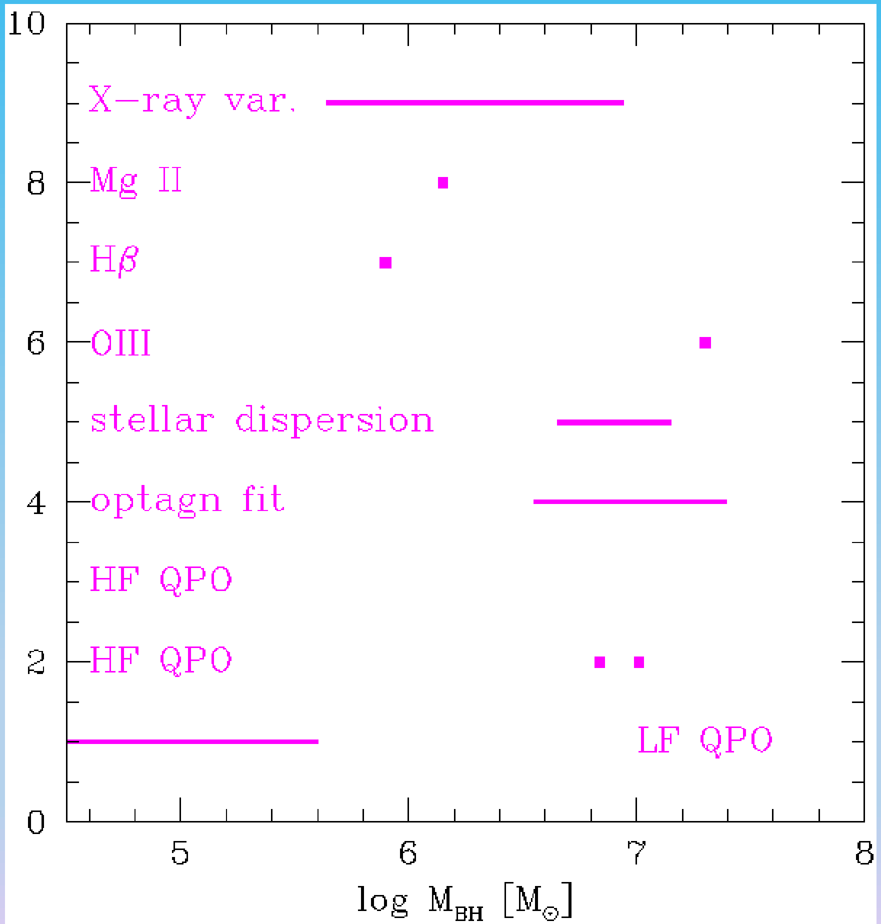

GRS 1915+105

RE J1034+396

rms(E)

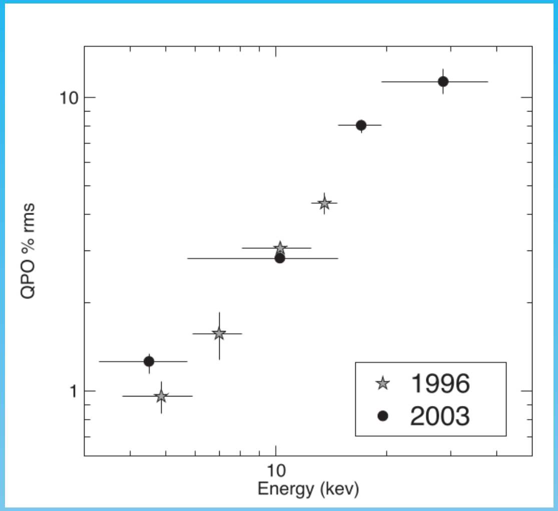

Belloni, Altamirano 2013

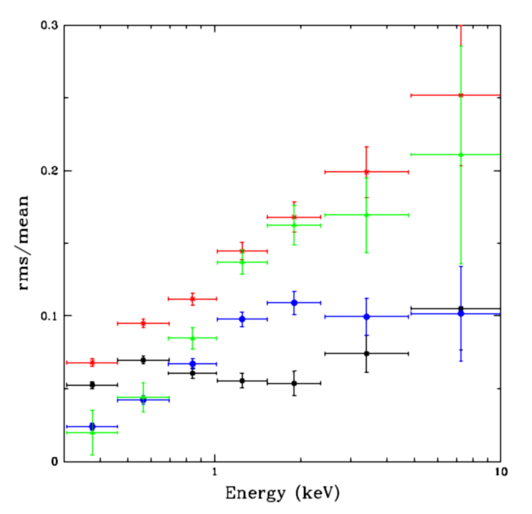

Middleton et al. 2009

Variations of the power law tail?

Thermal oscillations?

energy spectra

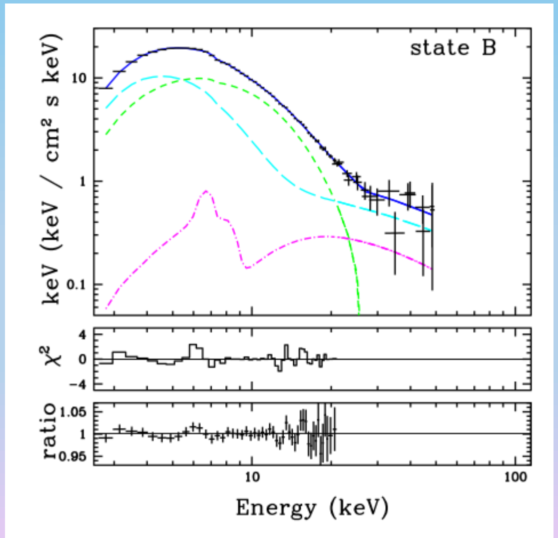

Sobolewska, Życki 2003

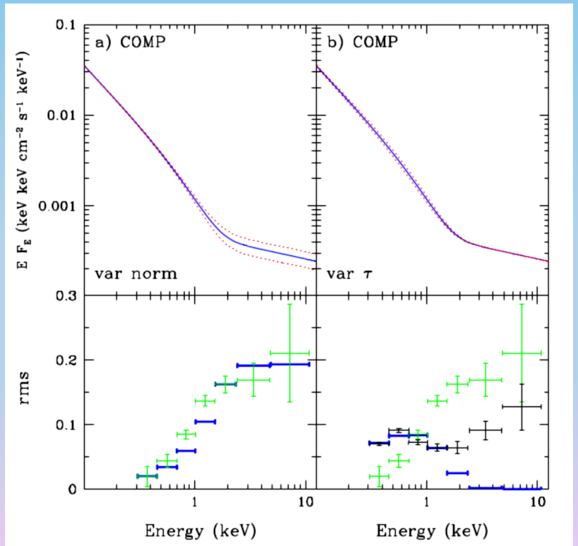

Low-frequency QPO in X-ray binaries

Data exist on spectral-temporal properties:

Disk emission not present in the QPO spectra – only the Comptonized component varies

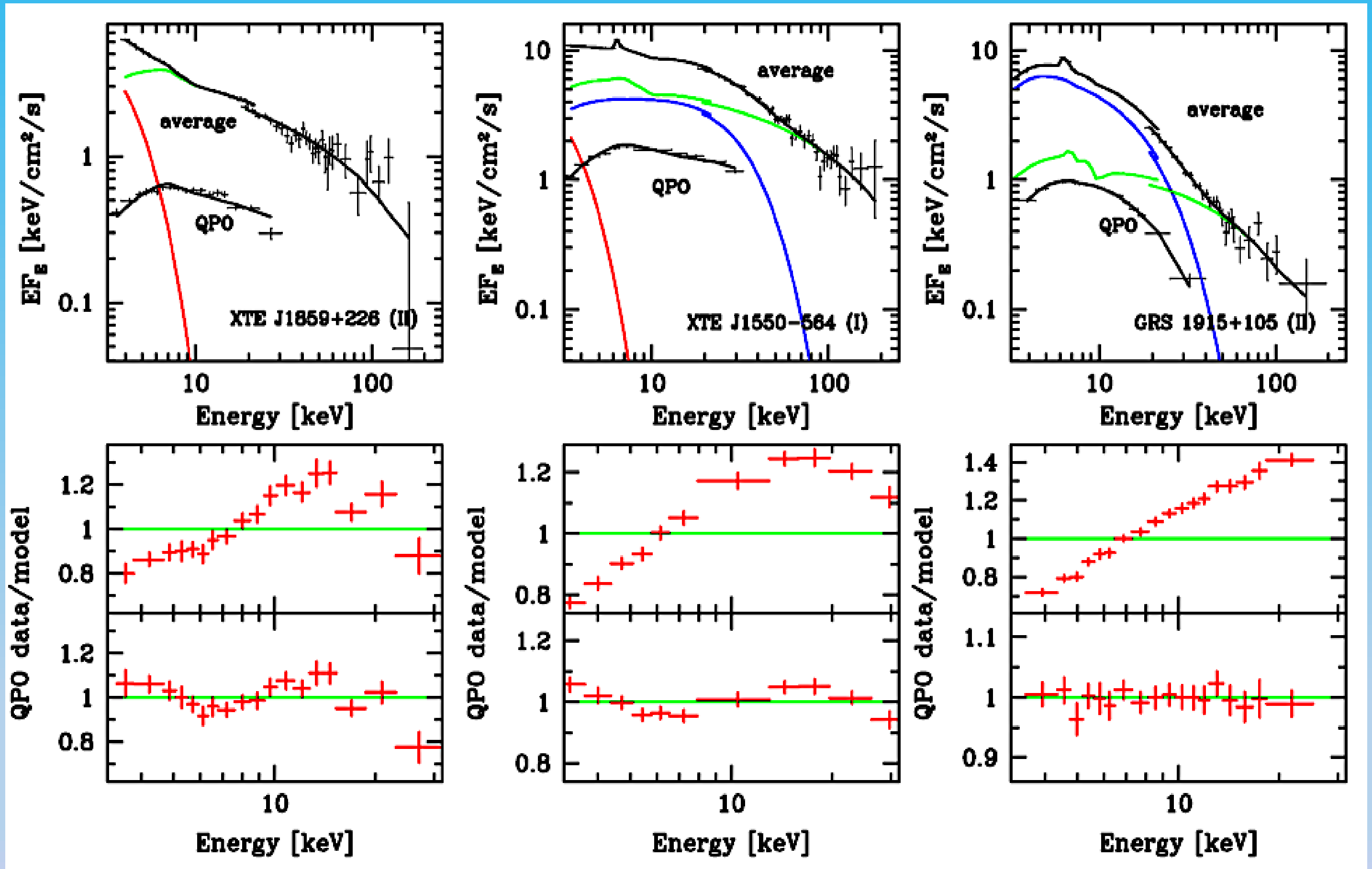

Sobolewska, Życki 2006

Geometry of the truncated disc

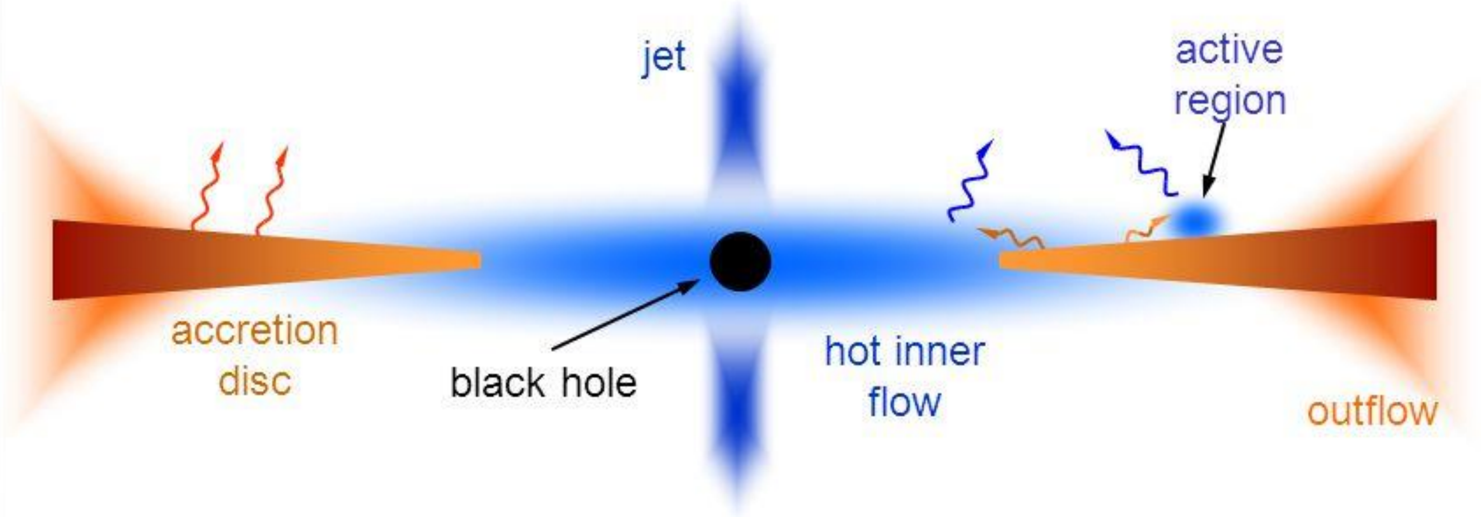

Marek Gierliński

X-ray spectra of XBR

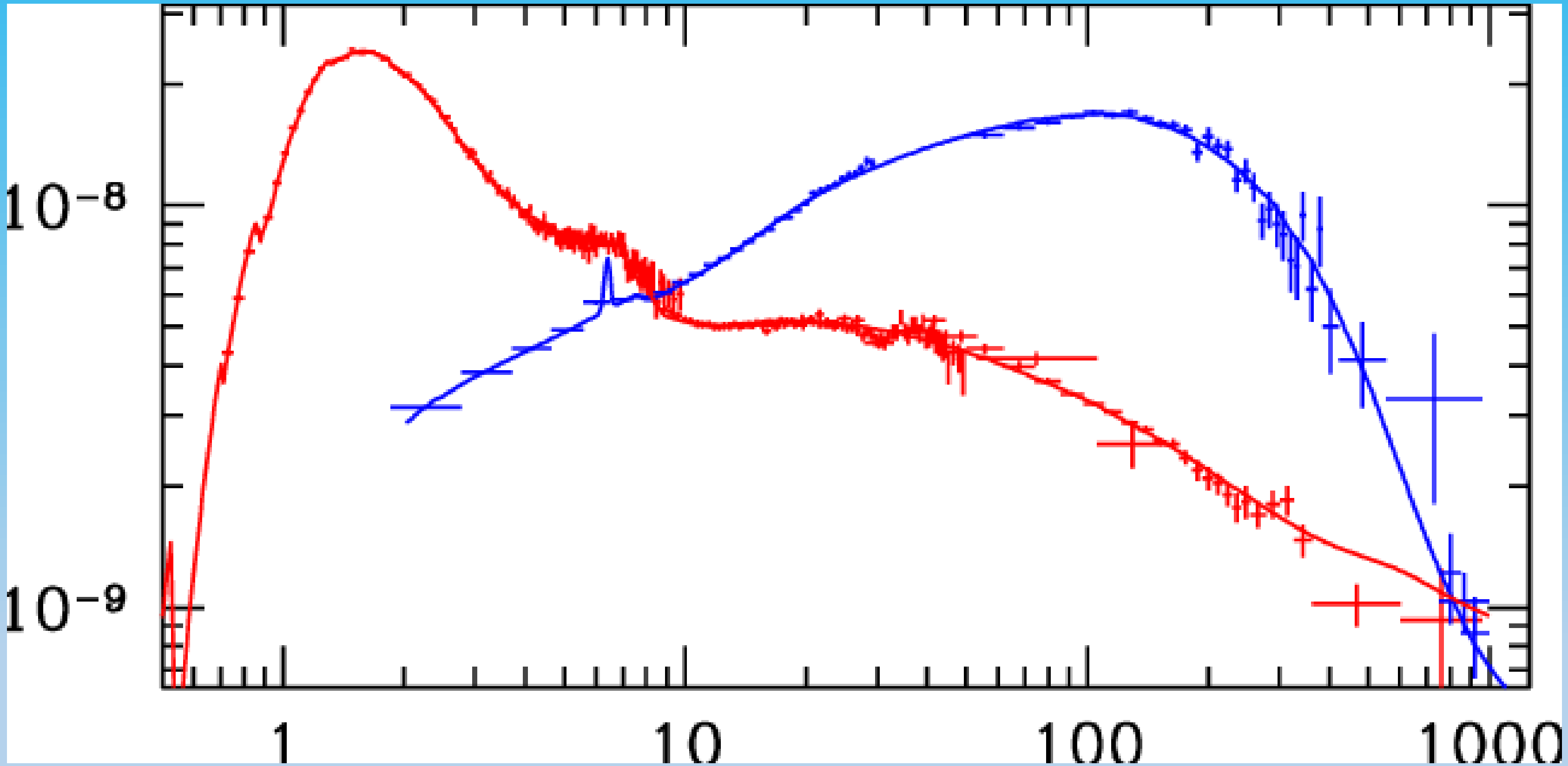

Gierlinski et al. 2008

Lense-Thirring precession model for low-*f* QPO

Formulated by Stella & Vietri (1998)

Recent hydrodynamical simulations suggest that the hot flow behaves (precesses) like a solid body.

Inner radius of the flow is determined by properties of the bending waves. It is approximately independent of the spin of the black hole. As a result the maximum precession frequency does not depend on the spin.

(C. Done, A. Ingram, C. Fragile)

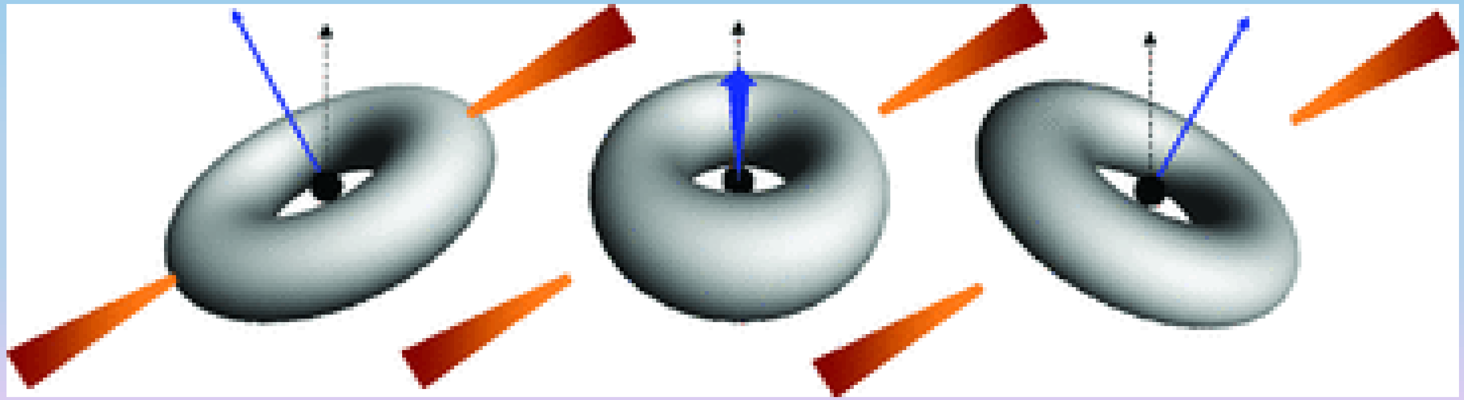

Simulating the spectra and time variability from this model

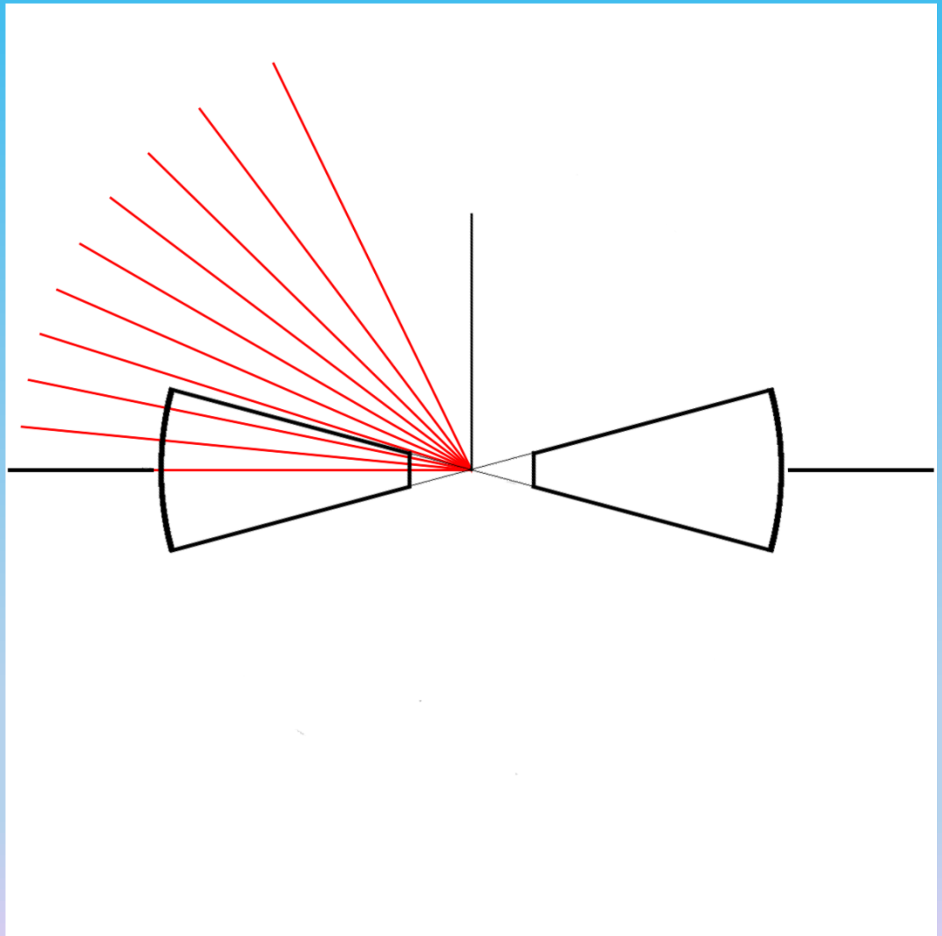

Simulating the spectra and time variability from this model

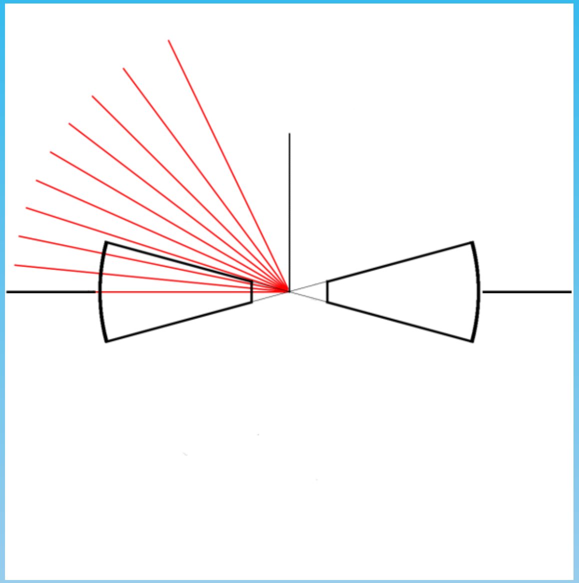

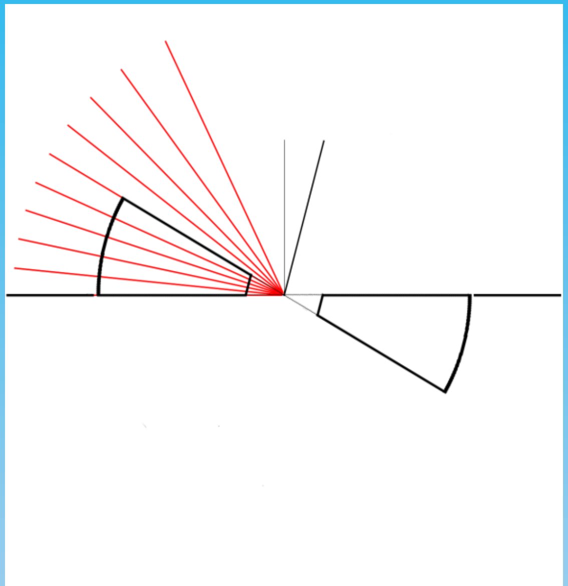

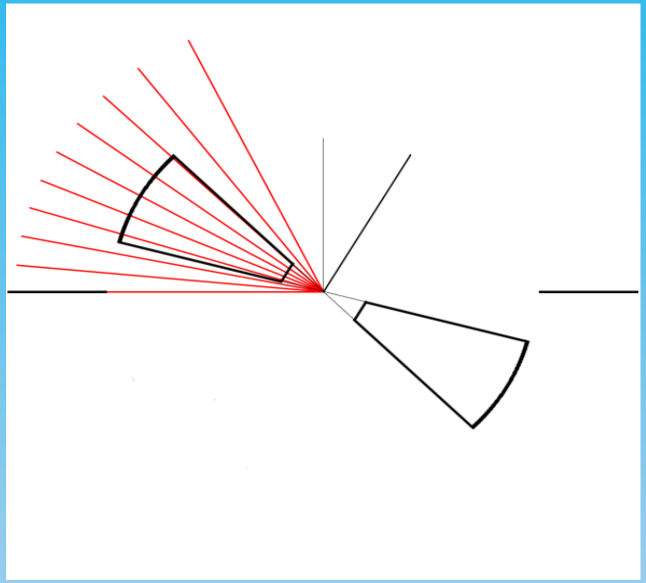

It’s a **3-D** situation!

As the hot torus precesses, the relative geometry of the torus and the outer cold disk changes, leading to a change of the soft photon fraction entering the hot torus, thus leading to variations of the hot plasma temperature. Additionally, the geometry of emitting torus, as observed from far away (red lines), changes

Geometry – reprocessing and relativistic effects

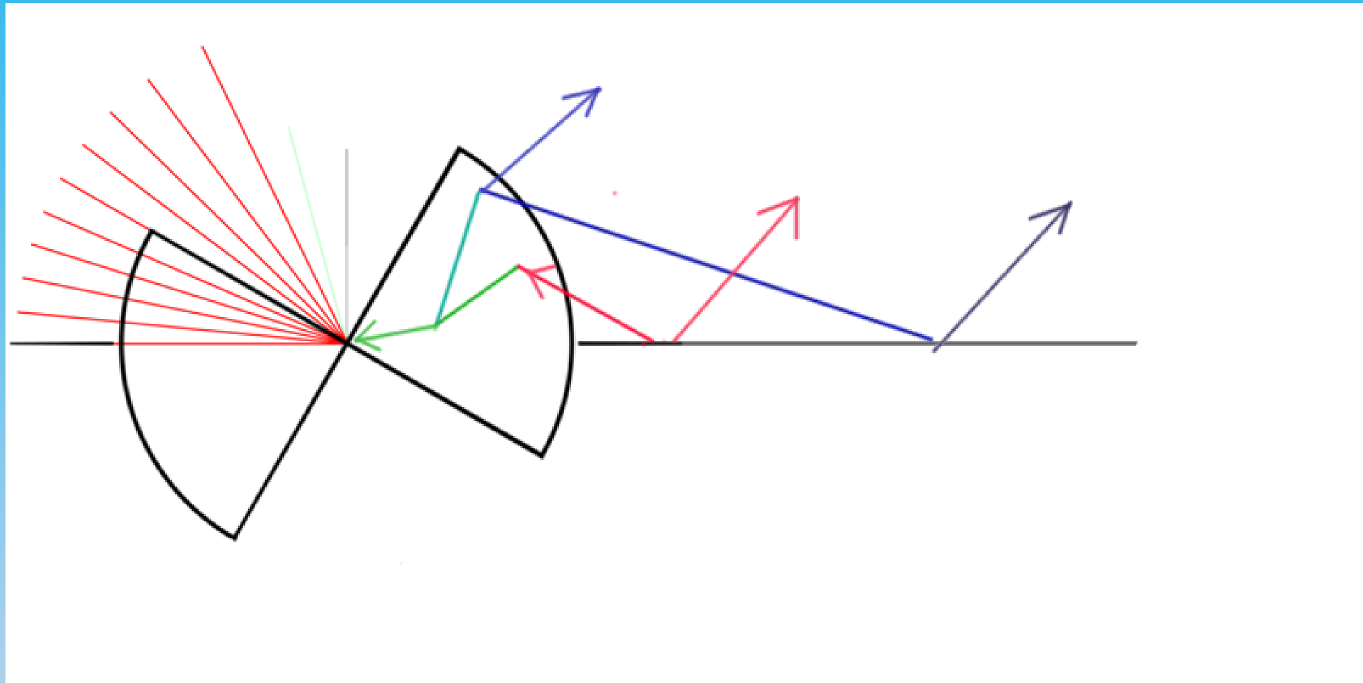

Relativistic ray-tracing applied on all coloured trajectories

Results – time averaged spectra

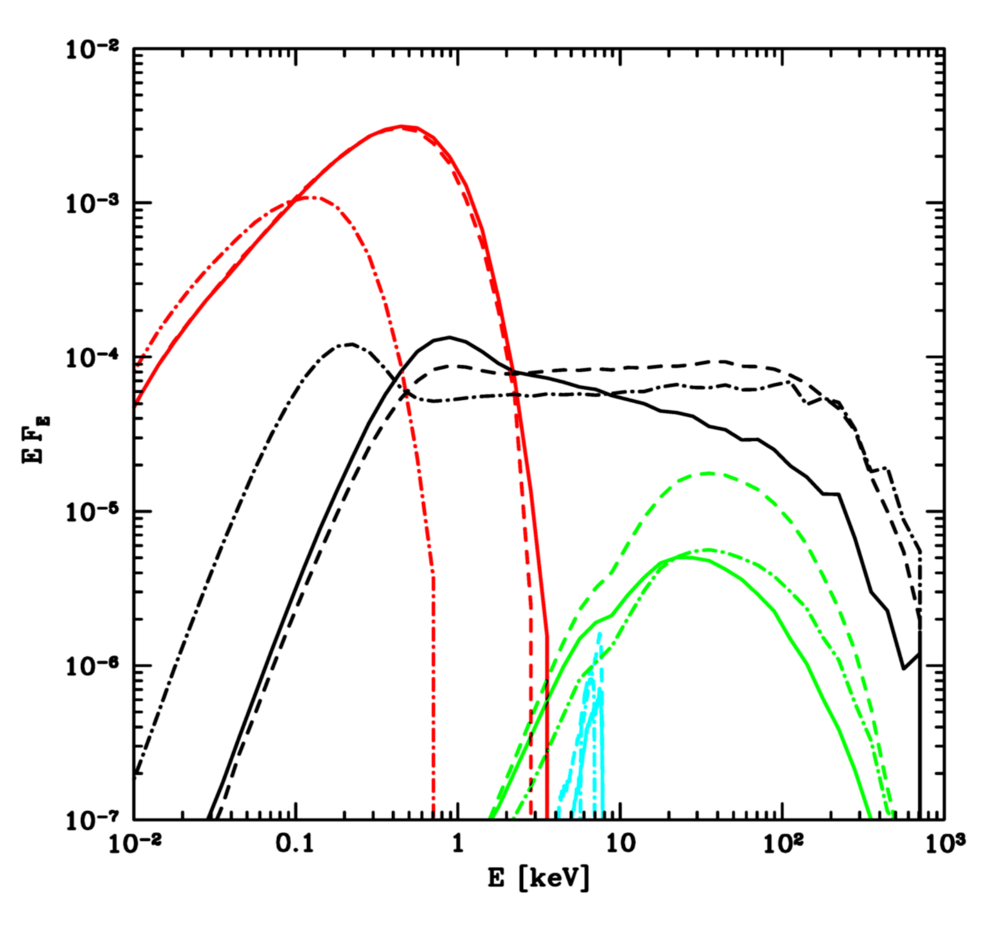

a=0.3, r_{tr}=10 (solid)

a=0.3, r_{tr}=90 (dash-dot)

a=0.9, r_{tr}=10 (dash)

Results – variations of the hot plasma temperature

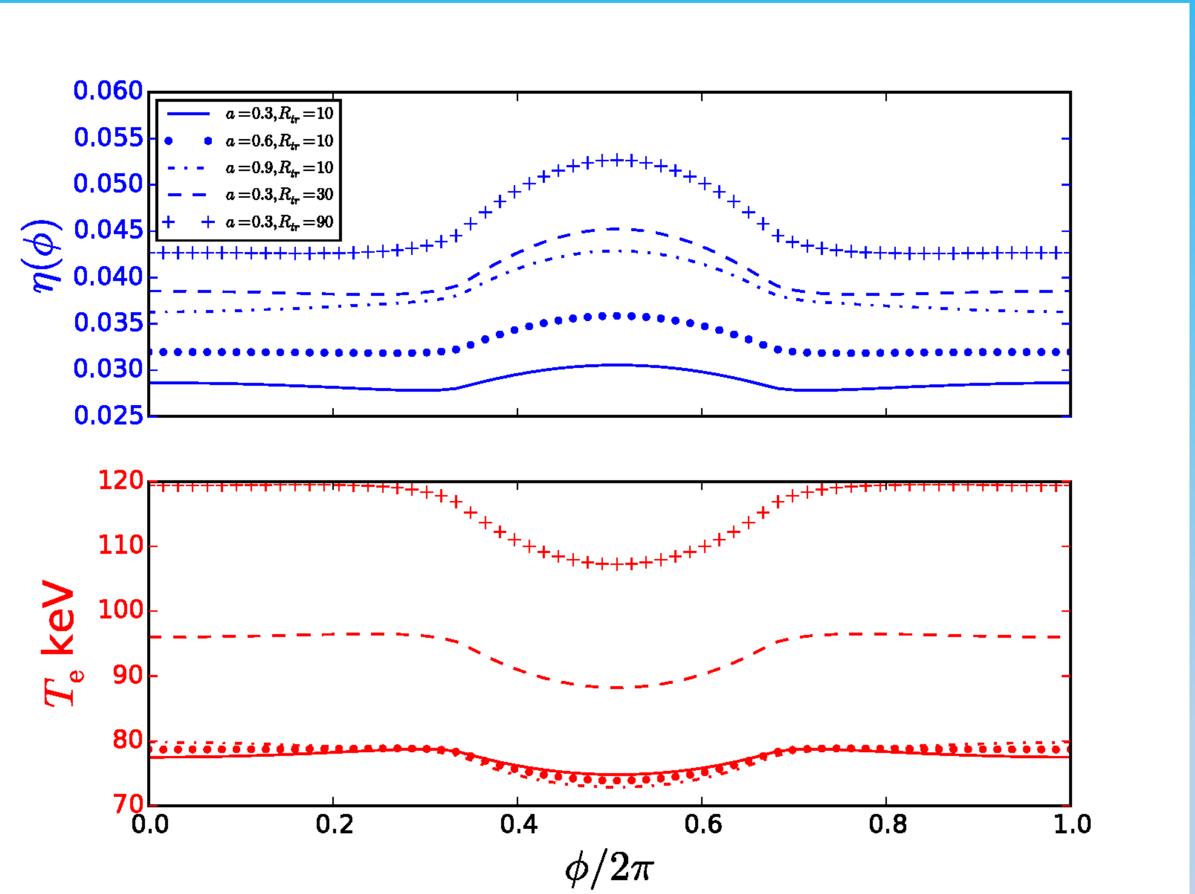

Fraction of the disk-emitted energy, intercepted by the torus

Electron temperature

You, Bursa, Życki 2018

Results – spectral variability

cos i=0.5, ϕ = 0

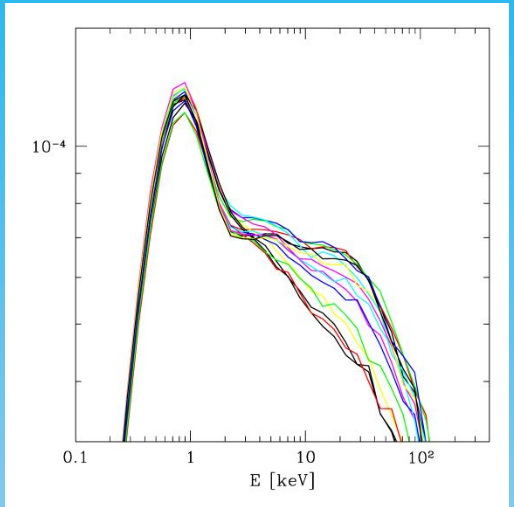

r_{tr}=10

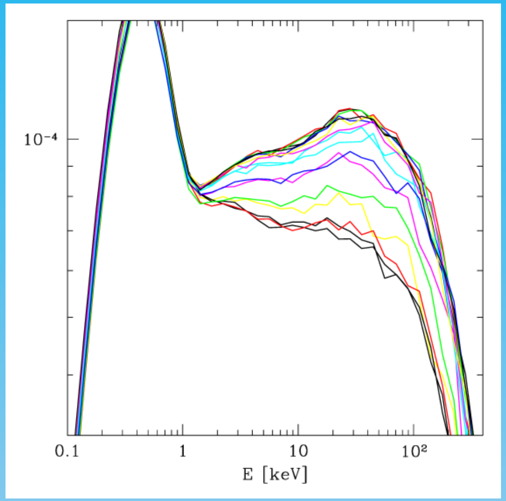

r_{tr}=30

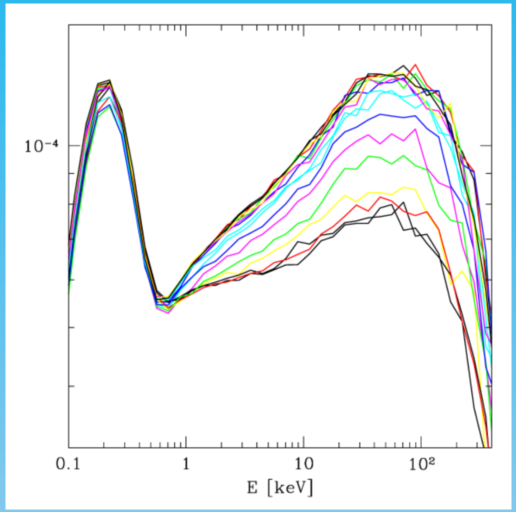

r_{tr}=90

a=0.3

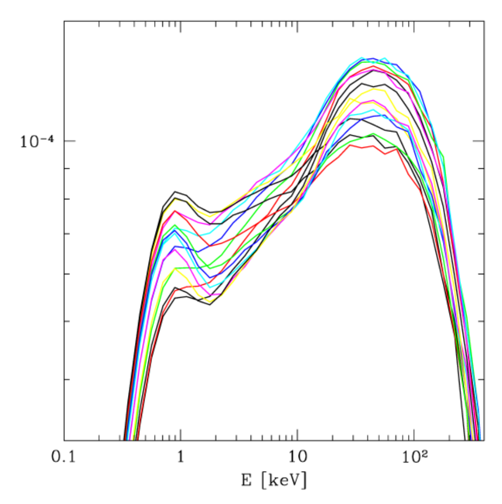

a=0.9

Spectral variability – rms(E)

a=0.3, r_{tr}=10

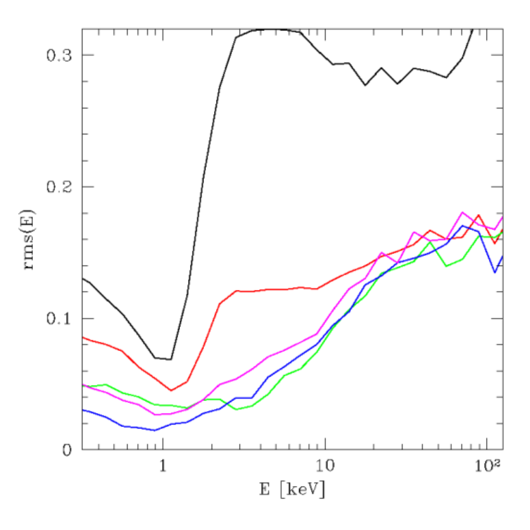

ϕ = 0 (towards observer)

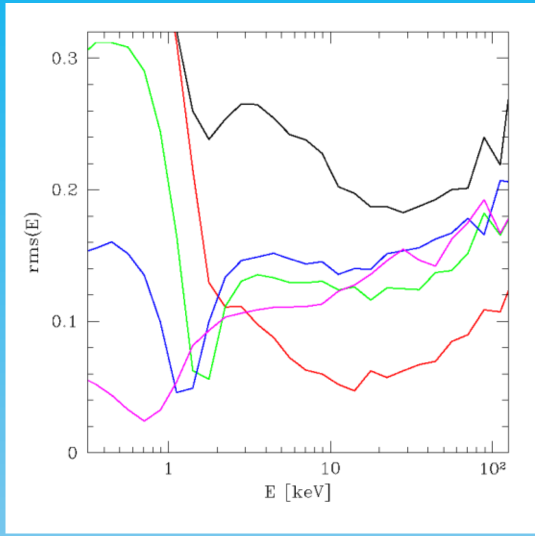

ϕ = 90

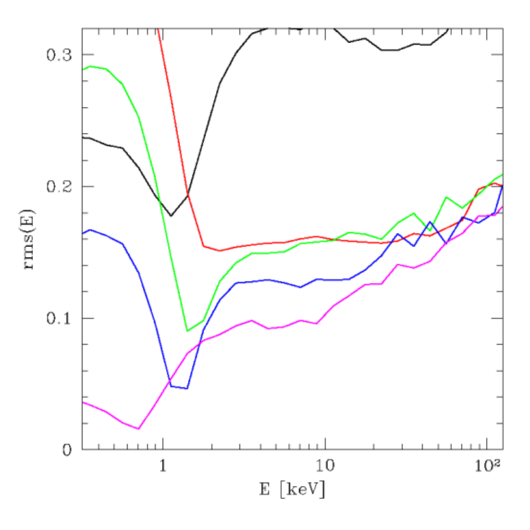

ϕ = 180 (away from observer)

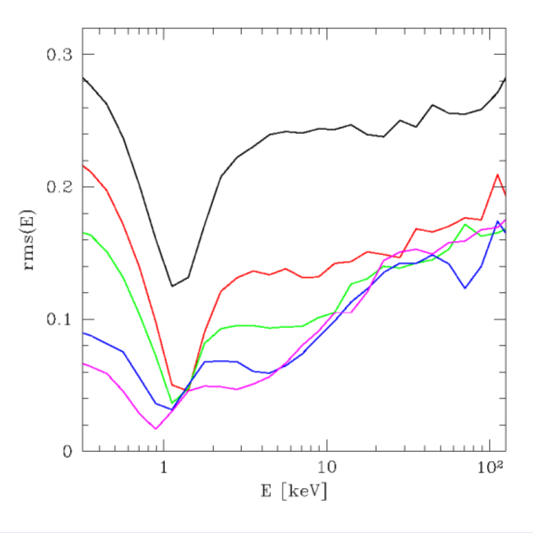

ϕ = 270

Fe K_α line variability

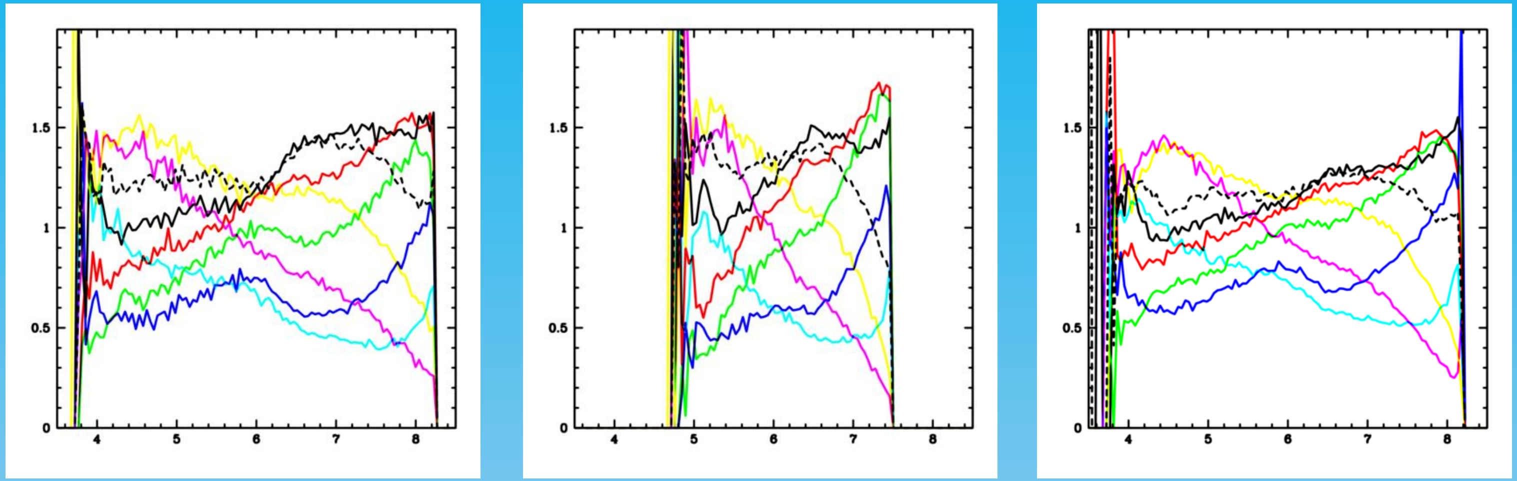

cos i=0.1

a=0.3, r_{tr}=10 **a=0.3, r_{tr}=30** **a=0.9, r_{tr}=10**

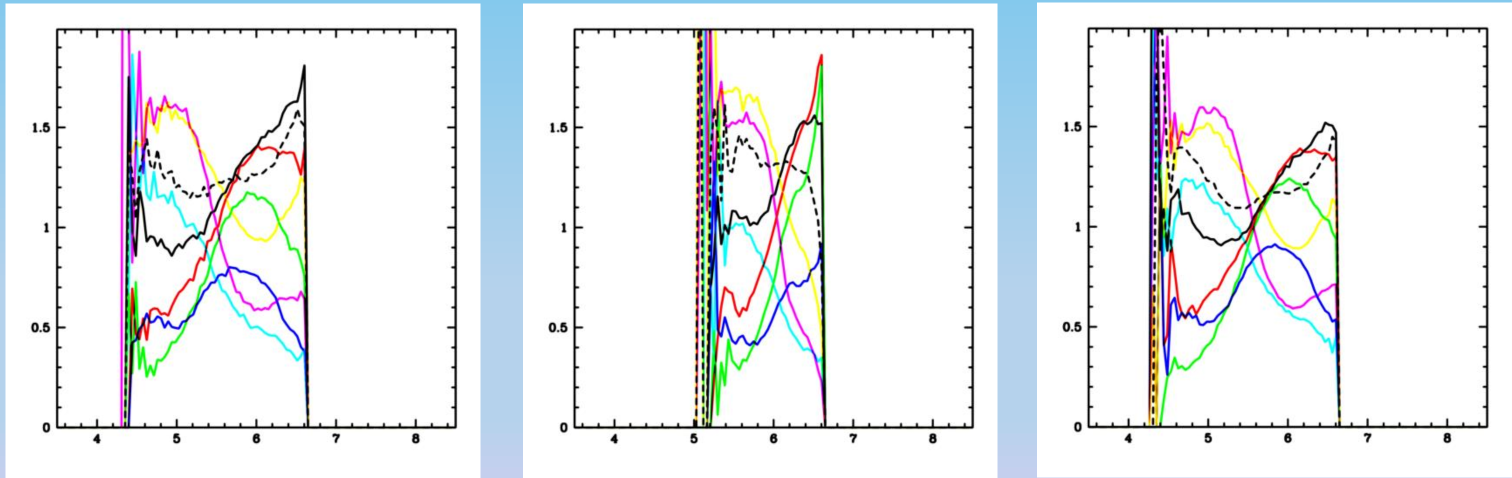

cos i = 0.9

AGN: TDE and QPO: ASASSN-14li

Pasham et al., 2019, Science

f ≈ 7.6 mHz

T ≈ 130 s

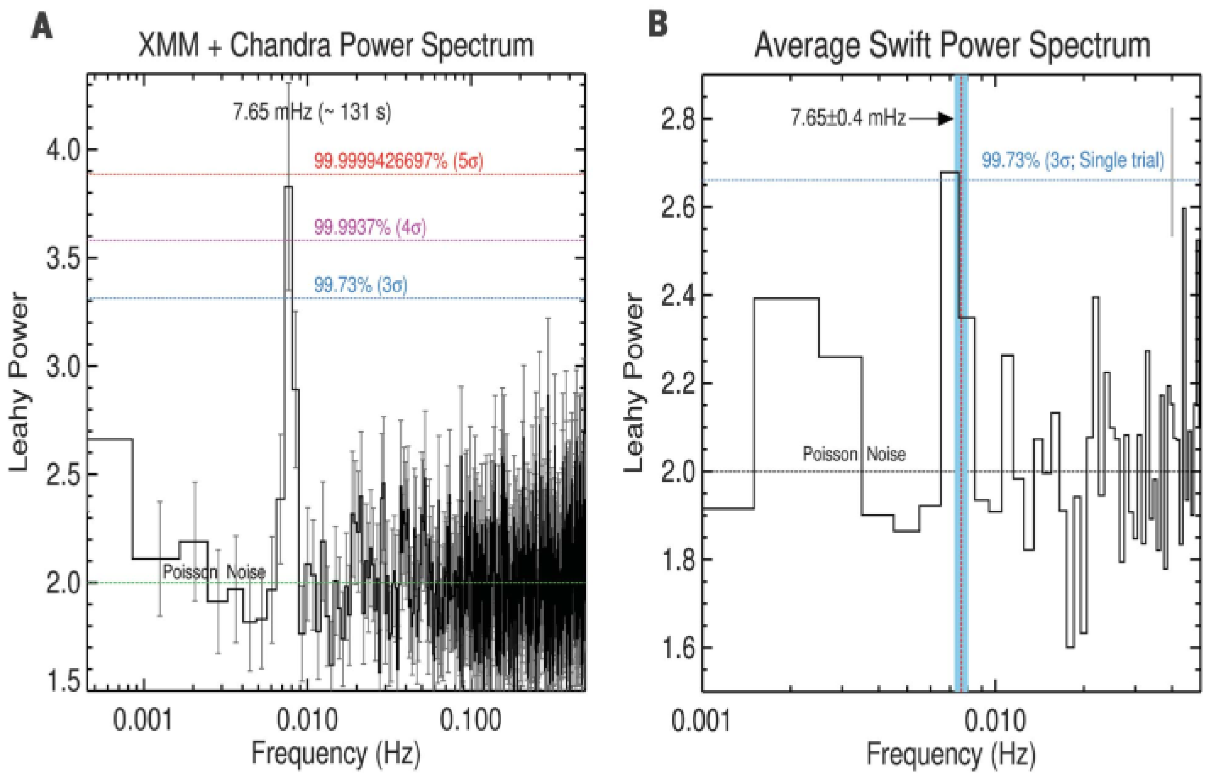

Fig. 2. X-ray power spectra for ASASSN-14li, showing a QPO at 7.65 mHz. (**A**) The average x-ray PDS from eight continuous 10,000-s light curves taken with XMM-Newton and Chandra. The frequency resolution is 0.8 mHz. The strongest feature in the power spectrum lies at a frequency of 7.65 ± 0.4 mHz (≈131 s). The horizontal blue, magenta, and red lines represent the 3, 4, and 5σ white-noise statistical thresholds. The data surrounding the QPO feature are consistent with white noise (*20*), but we also estimated the QPO significance under red noise, finding that its highest bin is significant at at least the 3.9σ level (*20*). Uncertainties of ±1σ are shown with gray error bars. Figure S9 shows the XMM-Newton and Chandra data separately. (**B**) Average Swift PDS from 85 continuous 1000-s light curves with a frequency resolution of 1 mHz. The blue horizontal line shows the 3σ threshold for a single trial search at 7.65 mHz. The highest peak in the power spectrum is at 7.0 ± 0.5 mHz, consistent with the XMM-Newton and Chandra power spectra (fig. S9).

Pasham *et al.*, *Science* **363**, 531–534 (2019)   1 February 2019   **2 of 4**

TDE and QPO: ASASSN-14li

Pasham et al., 2019, Science

f ≈ 7.6 mHz

T ≈ 130 s

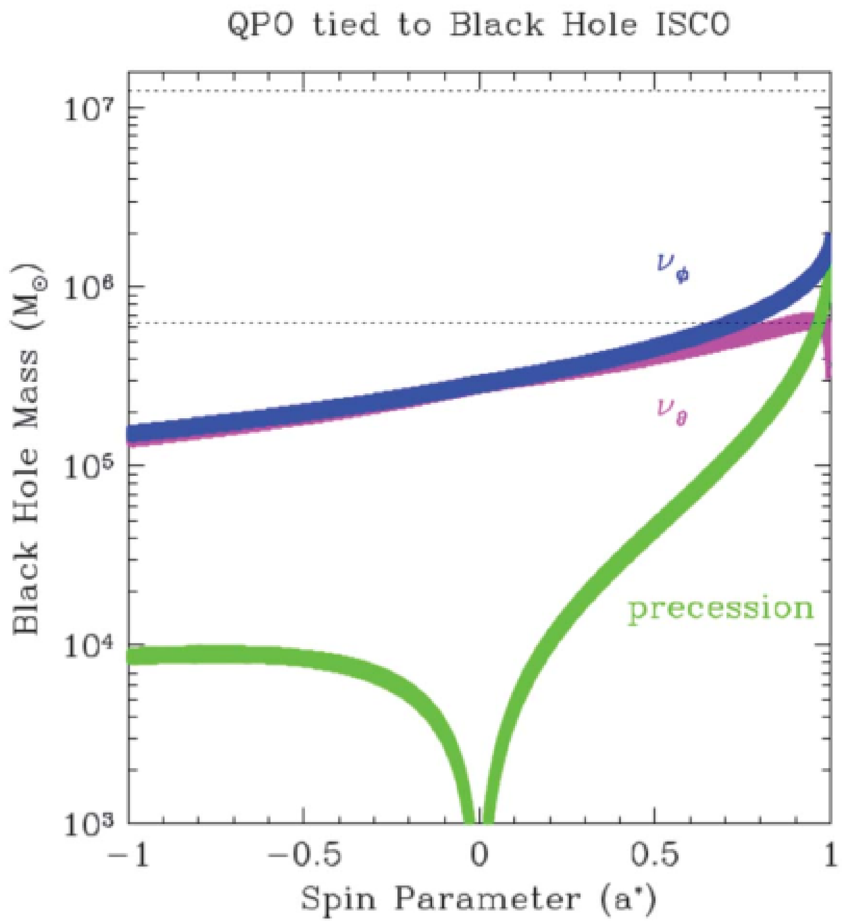

Fig. 4. BH dimensionless-spin-parameter–versus–mass contours. Spin-versus-mass contours determined by assuming that the 7.65-mHz QPO is associated with any of three particle frequencies—Keplerian frequency (ν_ϕ) (blue), vertical epicyclic frequency (ν_θ) (magenta), and Lense-Thirring precession ($\nu_\phi - \nu_\theta$) (green)—at the ISCO, where the radial epicyclic frequency (ν_r) is zero and the periastron precession frequency ($\nu_\phi - \nu_r$) is thus equal to the Keplerian frequency (*20*). The widths of these contours reflect the QPO's width of 0.7 mHz (upper limit). The dashed lines show ASASSN-14li's BH mass range ($10^{5.8}$ to $10^{7.1}$ $M_\odot$) estimated from its host galaxy scaling relations. Within this mass range, the only formal solutions are the ones that require the BH spin parameter to be greater than 0.7.

TDE and QPO: AT2020ocn/ZTF18aakelin

Pasham et al., 2024, Nature

$f \approx 7.8\times10^{-7}$ Hz
$T \approx 15$ days

Mass: **3×10^{6} M_{SUN}**

The mass is similar to RE J1034, but f_{QPO} very different

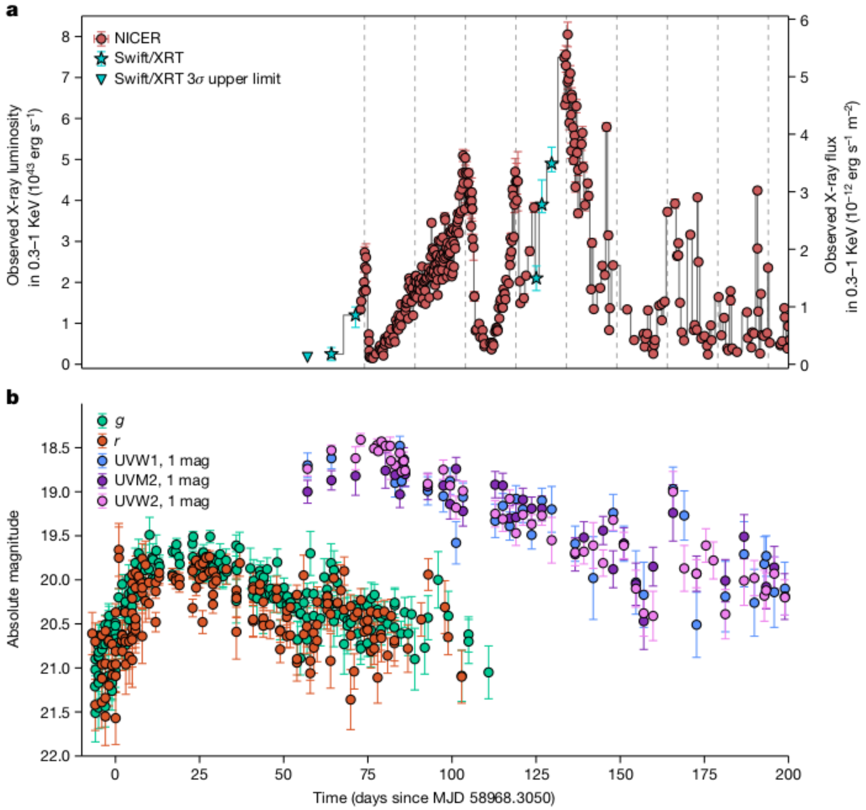

Fig. 1 | Multi-wavelength evolution of AT2020ocn. a, X-ray luminosity (0.3–1.0 keV) versus time since optical discovery. Gaps in NICER monitoring are filled by Swift data. The dashed and vertical lines are separated by 15 days to guide the eye. Archival Swift X-ray (0.3–1.0 keV) 3σ upper limits from before MJD 58274 is 3×10^{-14} erg s^{-1} cm^{-2} (4×10^{41} erg s^{-1}). The first X-ray or XRT data point is a non-detection with a 3σ upper limit of 1.7×10^{-13} erg s^{-1} cm^{-2}. **b**, Optical and UV evolution of AT2020ocn. All values are host-subtracted. All the other error bars represent 1σ uncertainties. See 'Data availability' section below to access the data.

TDE and QPO: AT2020ocn/ZTF18aakelin

Pasham et al., 2024, Nature

Fitting suggests that the QPO are due to variations of the temperature of the warm thermal component, but the X-ray data are good only up to 1 keV, so the harder spectral component is poorly constrained (is there a harder power law?)